Cloning and functional identification of slc5a12 as a sodium-coupled low-affinity transporter for monocarboxylates (SMCT2)

Sonne R. SRINIVAS*, Elangovan GOPAL†, Lina ZHUANG†, Shirou ITAGAKI†, Pamela M. MARTIN†, You-Jun FEI†, Vadivel GANAPATHY*† and Puttur D. PRASAD*†[1]

*Department of Obstetrics and Gynecology, Medical College of Georgia, Augusta, GA 30912, U.S.A., and †Department of Biochemistry and Molecular Biology, Medical College of Georgia, Augusta, GA 30912, U.S.A.

We report in the present paper, on the isolation and functional characterization of slc5a12, the twelfth member of the *SLC5* gene family, from mouse kidney. The slc5a12 cDNA codes for a protein of 619 amino acids. Heterologous expression of slc5a12 cDNA in mammalian cells induces Na^+-dependent transport of lactate and nicotinate. Several other short-chain monocarboxylates compete with nicotinate for the cDNA-induced transport process. Expression of slc5a12 in *Xenopus* oocytes induces electrogenic and Na^+-dependent transport of lactate, nicotinate, propionate and butyrate. The substrate specificity of slc5a12 is similar to that of slc5a8, an Na^+-coupled transporter for monocarboxylates. However, the substrate affinities of slc5a12 were much lower than those of slc5a8. slc5a12 mRNA is expressed in kidney, small intestine and skeletal muscle. *In situ* hybridization with sagittal sections of mouse kidney showed predominant expression of slc5a12 in the outer cortex. This is in contrast with slc5a8, which is expressed in the cortex as well as in the medulla. The physiological function of slc5a12 in the kidney is likely to mediate the reabsorption of lactate. In the intestinal tract, slc5a12 is expressed in the proximal parts, whereas slc5a8 is expressed in the distal parts. The expression of slc5a12 in the proximal parts of the intestinal tract, where there is minimal bacterial colonization, suggests that the physiological function of slc5a12 is not to mediate the absorption of short-chain monocarboxylates derived from bacterial fermentation but rather to mediate the absorption of diet-derived short-chain monocarboxylates. Based on the functional and structural similarities between slc5a8 and slc5a12, we suggest that the two transporters be designated as SMCT1 (sodium-coupled monocarboxylate transporter 1) and SMCT2 respectively.

Key words: cloning, functional characterization, low-affinity monocarboxylate transport, *SLC5*, sodium-coupled monocarboxylate transporter, *Xenopus laevis* oocyte.

INTRODUCTION

SLC5 is a solute-linked carrier gene family that contains sodium-coupled transporters for several nutrients. This gene family was originally thought to contain only 11 members (SLC5A1–SLC5A11) [1,2], but the recent GenBank® database shows the presence of an additional member (SLC5A12). The nutrients that are transported via the members of the *SLC5* family include glucose [SLC5A1/SGLT1 (sodium-dependent glucose transporter 1) and SLC5A2/SGLT2] [3,4], *myo*-inositol [SLC5A3/SMIT1 (sodium-dependent *myo*-inositol transporter 1) and SLC5A11/SMIT2] [5,6], iodide [SLC5A5/NIS (Na^+/iodide co-transporter)] [7], biotin and pantothenate [SLC5A6/SMVT (sodium-coupled multivitamin transporter)] [8], choline [SLC5A7/CHT1 (choline transporter 1)] [9], short-chain fatty acids/lactate/nicotinate [SLC5A8/SMCT, where SMCT stands for sodium-coupled MCT (monocarboxylate transporter)] [10] and mannose (SLC5A9) [11]. One member of the family (SLC5A4) functions as a glucose-sensitive Na^+ channel rather than as a sodium-coupled transporter [12]. The functional identity of two of the family members (SLC5A10 and SLC5A12) has not yet been established.

The recent functional identification of SLC5A8 as a sodium-coupled transporter for lactate, short-chain fatty acids (acetate, propionate and butyrate) and nicotinate [13–16] has provided the molecular basis of active absorption of these nutrients in the kidney and intestinal tract. Lactate is actively reabsorbed in the kidney by an Na^+-coupled transport mechanism [17,18]. The Na^+-independent transport process for lactate, mediated by the H^+-coupled MCTs, does not play any role in this process [19]. However, studies by Jorgensen and Sheikh [20] have shown that there are two distinct transport systems for lactate in the kidney, one being a low-affinity system found in the superficial cortex and the other being a high-affinity system found in the outer medulla. Plasma levels of lactate under normal physiological conditions are approx. 1.5 mM [21], but there is no or little excretion of lactate in urine, suggesting efficient reabsorption in the kidney. The expression of a low-affinity system in the initial portions of the nephron enables effective reabsorption of lactate at relatively high concentrations. As the reabsorption continues along the proximal portions of the nephron, the tubular concentrations decrease. The expression of a high-affinity system in the latter portions of the nephron enables effective reabsorption at these relatively lower concentrations. *In situ* hybridization studies have shown that the recently identified sodium-coupled transporter for lactate/monocarboxylates (SMCT) is expressed in the cortex as well as medulla, indicating that the transporter may represent the high-affinity lactate transport system [15]. The Michaelis constant for lactate for transport via SMCT

Abbreviations used: HPRT, hypoxanthine–guanine phosphoribosyltransferase; HRPE, human retinal pigment epithelial; MCT, monocarboxylate transporter; NIS, Na^+/iodide co-transporter; NMDG, *N*-methyl-D-glucamine; poly(A)$^+$ RNA, polyadenylated RNA; RT, reverse transcriptase; SGLT, sodium-dependent glucose transporter; SMCT, sodium-coupled MCT; SMIT, sodium-dependent *myo*-inositol transporter; SMVT, sodium-coupled multivitamin transporter.

[1] To whom correspondence should be addressed (email pprasad@mail.mcg.edu).

The nucleotide sequence data reported will appear in GenBank®, EMBL, DDBJ and GSDB Nucleotide Sequence Databases under the accession number AY964639.

is approx. 0.25 mM, which agrees well with the Michaelis constant for lactate transport via the high-affinity transport system described in the kidney [20]. The molecular identity of the low-affinity transport system for lactate in the kidney has remained unknown. In the present paper, we describe the cloning and functional identification of slc5a12 as a sodium-coupled low-affinity transporter for lactate. In addition to lactate, the newly identified transporter also transports short-chain fatty acids and nicotinate. Thus slc5a12 is very similar to slc5a8 in substrate selectivity and Na^+ dependence. A major difference between the two transporters lies in the relative affinity for their substrates, slc5a8 being a high-affinity transporter and slc5a12 being a low-affinity transporter. Based on these findings, we designate slc5a12 as SMCT2 and rename slc5a8 as SMCT1. slc5a12 is expressed predominantly in the cortical portion of the kidney, agreeing with the already known location of the low-affinity transport system for lactate.

EXPERIMENTAL

Cloning of the mouse slc5a12 cDNA

A cDNA library, constructed in the pSPORT1 vector using the SuperScript System for cDNA cloning (Invitrogen, Carlsbad, CA, U.S.A.) and poly(A)$^+$ RNA (polyadenylated RNA) isolated from mouse kidney, was used for screening. The rat SMVT (slc5a6) cDNA [22], labelled with [α-^{32}P]dCTP by random priming using the Ready-to-go oligolabelling beads (Amersham Biosciences, Piscataway, NJ, U.S.A.), was used as the probe. Screening was done under medium stringency conditions [22,23]. Sequencing of both strands of the cDNA was performed using an automated PerkinElmer Applied Biosystems (Foster City, CA, U.S.A.) 377 Prism DNA sequencer.

Functional characterization of mouse slc5a12 in mammalian cells

The cloned slc5a12 cDNA was expressed in HRPE (human retinal pigment epithelial) cells using the vaccinia virus-mediated expression system [15,16]. Subconfluent HRPE cells were infected with the recombinant (VTF_{7-3}) vaccinia virus encoding T7 polymerase and then transfected with the plasmid carrying the full-length cDNA. Uptake of [^{14}C]lactate (specific radioactivity, 150 mCi/mmol) and [^{14}C]nicotinate (specific radioactivity, 55 mCi/mmol) (American Radiolabeled Chemicals, St. Louis, MO, U.S.A.) was measured with a 15 min incubation at 37 °C 12–15 h post-transfection. HRPE cells transfected with the empty vector were used to measure endogenous transport activity. Uptake measurements in vector- and cDNA-transfected cells were always done in parallel under identical experimental conditions. The slc5a12-specific transport was determined by subtracting the transport values measured in vector-transfected cells from the transport values measured in cDNA-transfected cells. The uptake buffer was 25 mM Hepes/Tris (pH 7.5), containing 140 mM NaCl, 5.4 mM KCl, 1.8 mM $CaCl_2$, 0.8 mM $MgSO_4$ and 5 mM glucose. When transport measurements were made in the absence of Na^+, NaCl in the uptake buffer was replaced with an equimolar concentration of NMDG (*N*-methyl-D-glucamine) chloride. When uptake of lactate was measured, α-cyano-4-hydroxycinnamate (5 mM), a specific inhibitor of MCTs [24,25], was included in the uptake buffer to block the MCT-mediated uptake. When substrate concentrations of more than 5 mM were used in inhibition studies, an equimolar concentration of NaCl in the uptake buffer was replaced by the sodium salt of the substrate being tested. This was done to maintain the osmolarity of the buffer. In dose–response studies where high concentrations of substrates as sodium salts were used, the concentration of NaCl in the uptake buffer was held constant at 40 mM and osmolarity of the uptake buffer was maintained by the addition of appropriate concentrations of sodium gluconate. Uptake measurements were made in triplicate and experiments were repeated at least three times. Results are presented as the means $\pm$ S.E.M. for these replicates.

Functional characterization of mouse slc5a12 following heterologous expression in *Xenopus laevis* oocytes

Capped cRNA from slc5a12 cDNA was synthesized using the mMESSAGE mMACHINE kit according to the manufacturer's (Ambion, Austin, TX, U.S.A.) instructions. Mature oocytes were isolated from *X. laevis* by manual defolliculation and injected with 50 ng of cRNA/oocyte. Oocytes injected with slc5a8 cRNA encoding the recently characterized sodium-dependent MCT served as positive controls and oocytes injected with water were used to determine endogenous transport activity. Electrophysiological studies were done 5–6 days after cRNA injection by the conventional two-microelectrode voltage-clamp method [16]. Perfusion buffers containing the same concentration of Na^+ but different concentrations of substrates were prepared by mixing buffers containing 100 mM NaCl, 100 mM sodium gluconate, or 100 mM of the sodium salt of individual substrates in 2 mM KCl, 1 mM $MgCl_2$, 1 mM $CaCl_2$ and 10 mM Hepes, titrated to pH 7.5 with Tris. While the concentration of Na^+ remained constant in these experiments, the concentration of Cl^- varied between 0 and 50 mM depending on the concentration of the substrate used. To rule out possible artifacts in electrophysiological measurements due to changes in Cl^- concentration, the oocytes were first equilibrated with a buffer in which the sodium salt of the substrate was replaced with equimolar amounts of sodium gluconate until the current recordings reached the baseline before perfusing with the substrate-containing buffer. In between the measurements, the oocyte was perfused with ND-96 buffer (96 mM NaCl, 2 mM KCl, 1.8 mM $CaCl_2$, 1 mM $MgCl_2$ and 5 mM Hepes, titrated with NaOH to pH 7.4). In all experiments, the membrane potential was clamped at -50 mV and the difference between the steady-state currents measured in the presence and absence of substrates was considered as the substrate-induced current.

Water-injected and slc5a12 cRNA-injected oocytes (5–6 days following injection) were also used for measurement of lactate. Oocytes (8–10 oocytes/assay) were incubated in 250 μl of uptake buffer containing 3 μCi of [^{14}C]lactate. The concentration of lactate was 5 mM (labelled plus unlabelled). Uptake measurements were carried out for 1 h in the presence or absence of Na^+ using the buffers described for the electrophysiological studies. Following 1 h incubation, the uptake medium was removed and the oocytes were washed three times with ice-cold buffer. Radioactivity associated with individual oocytes was then counted as described previously [15]. Endogenous uptake activity for lactate in water-injected oocytes was monitored in a similar manner in the presence or absence of Na^+. These measurements were made either on day 2 or on day 5 following oocyte isolation.

Determination of tissue-specific expression of slc5a12

Tissue distribution of slc5a12 mRNA was determined by Northern-blot analysis and RT–PCR (where RT stands for reverse transcriptase). For Northern-blot analysis, a commercially (Origene, Rockville, MD, U.S.A.) available blot containing poly(A)$^+$ RNA from several mouse tissues and a second home-made blot containing poly(A)$^+$ RNA from small intestine and

Table 1 Primers used for RT–PCR analysis of mouse slc5a8, slc5a12 and HPRT1

Gene	Primer sequence	Position	Expected size	GenBank® accession no.
slc5a8	Sense: 5′-TTATGGGCGGTCGCAGTA-3′	452–469	725 bp	AY484428
	Antisense: 5′-CAGAGGCCCACAAGGTTGACAT-3′	1178–1157		
slc5a12	Sense: 5′-TTGGCCCTGTAGCTTTGTCTCTG-3′	155–177	858 bp	AY964639
	Antisense: 5′-AAGTCCTGGCAGCCCTGGCATAGT-3′	1014–991		
HPRT1	Sense: 5′-GCGTCGTGATTAGCGATGATGAAC-3′	107–130	155 bp	NM_013556
	Antisense: 5′-CCTCCCATCTCCTTCATGACATCT-3′	263–240		

colon were used. The blots were probed with ^{32}P-labelled slc5a12 cDNA. The hybridization and post-hybridization washes were done under high-stringency conditions as described previously [8,22]. For RT–PCR analysis, total RNA was isolated from several mouse tissues using TRIzol® reagent. Total RNA (1 μg) was reverse transcribed using Superscript II-RT (Invitrogen) and random hexamers according to the manufacturer's instructions. A standard PCR reaction with 100 pmol of each primer and a 2 μl aliquot of the RT reaction was used for amplification of the fragments. Primers specific for mouse HPRT1 (hypoxanthine–guanine phosphoribosyltransferase 1) were also included in each reaction as an internal control. The nucleotide sequences of the primers, their position and expected sizes are given in Table 1. Amplification involved 35 cycles at 94 °C, 30 s; at 59 °C, 30 s; at 72 °C, 2 min; and a final extension at 72 °C for 30 min in a thermocycler using Platinum Taq polymerase (Invitrogen).

In situ hybridization

The regional distribution of slc5a12 transcripts in the kidney was determined by *in situ* hybridization in sagittal cryosections of mouse kidney as described previously [15]. For the preparation of antisense and sense (negative control) riboprobes, a 541 bp EcoRI–BamHI fragment, which corresponds to nt 124–664 of the slc5a12 cDNA, was cloned into pSPORT1 plasmid. The probes were prepared by *in vitro* transcription using the DIG nucleic acid detection kit (Roche Diagnostics, Indianapolis, IN, U.S.A.) with appropriate RNA polymerases (T7 RNA polymerase for the sense probe and SP6 RNA polymerase for the antisense probe) after linearizing the plasmid with BamHI for the sense probe and EcoRI for the antisense probe. Tissue sections were permeabilized with proteinase K (1 mg/ml) in PBS for 4 min. The proteinase K activity was stopped by rinsing the slides in glycine (2 mg/ml) in PBS. Sections were washed in PBS, equilibrated in 5 % SSC (1 × SSC is 0.15 M NaCl/0.015 M sodium citrate, pH 7) and prehybridized for 2 h at 58 °C in 50 % (v/v) formamide, 5 % SSC, 2 % (w/v) blocking reagent (provided with the DIG nucleic acid detection kit), 0.1 % (w/v) *N*-lauroylsarcosine and 0.02 % (w/v) SDS. Sections were hybridized with the probes (1 μg/ml) under high-stringency conditions and incubated overnight at 58 °C. They were washed twice in 2 % SSC at 25 °C, twice in 1 % SSC at 55 °C and twice in 0.1 % SSC at 37 °C. For immunological detection of the probe, sections were washed in a buffer containing 0.1 M maleic acid and 0.15 M NaCl (pH 7.5) and blocked with the same buffer containing 1 % blocking reagent. The anti-digoxigenin antibody conjugated with alkaline phosphatase was diluted 1:5000 and slides were incubated with this antibody for 2 h at 25 °C. Sections were washed twice in the preceding wash buffer containing levamisol (200 mg/ml) for 10 min and equilibrated with a buffer containing 100 mM Tris/HCl (pH 9.5), 100 mM NaCl and 50 mM $MgCl_2$. The colour reaction was developed using the chromogenic substrate Nitro Blue Tetrazolium/5-bromo-4-chloro-3-indolyl phosphate. Slides were washed in distilled water and coverslips were applied, but the sections were not counter-stained so that the purplish-red coloured precipitate, indicative of a positive reaction, could be visualized in the sections. In all cases, some sections were hybridized with the sense probe to determine non-specific binding.

Semi-quantitative RT–PCR

The distribution of slc5a12 transcripts along the length of the intestinal tract in mice was determined by semi-quantitative RT–PCR. The entire length of the small intestine, from duodenum to ileum, was dissected out and cut into three equal-length segments. RNA was prepared from these three segments using TRIzol® reagent. In addition, total RNA was also isolated from the caecum and colon. Reverse transcription was carried out using murine leukaemia virus RT according to the manufacturer's (Roche Molecular Systems, Branchburg, NJ, U.S.A.) instructions. Multiplexed PCR reactions were set up as described earlier with 300 pmol of primers specific for slc5a12 and HPRT1, the latter serving as an internal control, and 2 μl aliquot of cDNA. In order to compare the expression of slc5a12 with that of slc5a8, simultaneous reactions were set up in which slc5a12-specific primers were replaced by slc5a8-specific primers. The PCR method consisted of 25 cycles of denaturing at 94 °C for 30 s, annealing at 59 °C for 30 s and extension at 72 °C for 60 s, followed by a final extension at 72 °C for 30 min. The resultant PCR products were size-fractionated in agarose gels, stained with ethidium bromide and the intensities of the bands were measured by densitometry using a SpectraImager 5000 Imaging system and AlphaEase 32-bit software (Alpha Innotech, San Leandro, CA, U.S.A.).

RESULTS

Structural features of mouse slc5a12 cDNA

The screening of the mouse kidney cDNA library with a mouse slc5a6 (SMVT)-specific cDNA probe yielded two cDNA clones that were different from slc5a6. One of them turned out to be slc5a8, the characterization of which was published in an earlier report from our laboratory [15]. The second cDNA, which is 3235 bp-long with an open reading frame of 1860 bp encoding a protein of 619 amino acids, is slc5a12. The open reading frame is flanked by a 5′-non-coding sequence of 6 bp and a 1369 bp-long 3′-non-coding sequence. The sequence has been deposited in the GenBank® database (accession no. AY964639). The slc5a12-encoded protein is highly hydrophobic with 13 putative transmembrane domains with the N-terminus at the exoplasmic side of the membrane and the C-terminus at the cytoplasmic side of the membrane. With this topology model, mouse slc5a12 has two putative N-glycosylation sites, between transmembrane domains 6 and 7 (Asn^{219}) and transmembrane domains 12 and 13 (Asn^{480}). The deduced amino acid sequence also displays putative

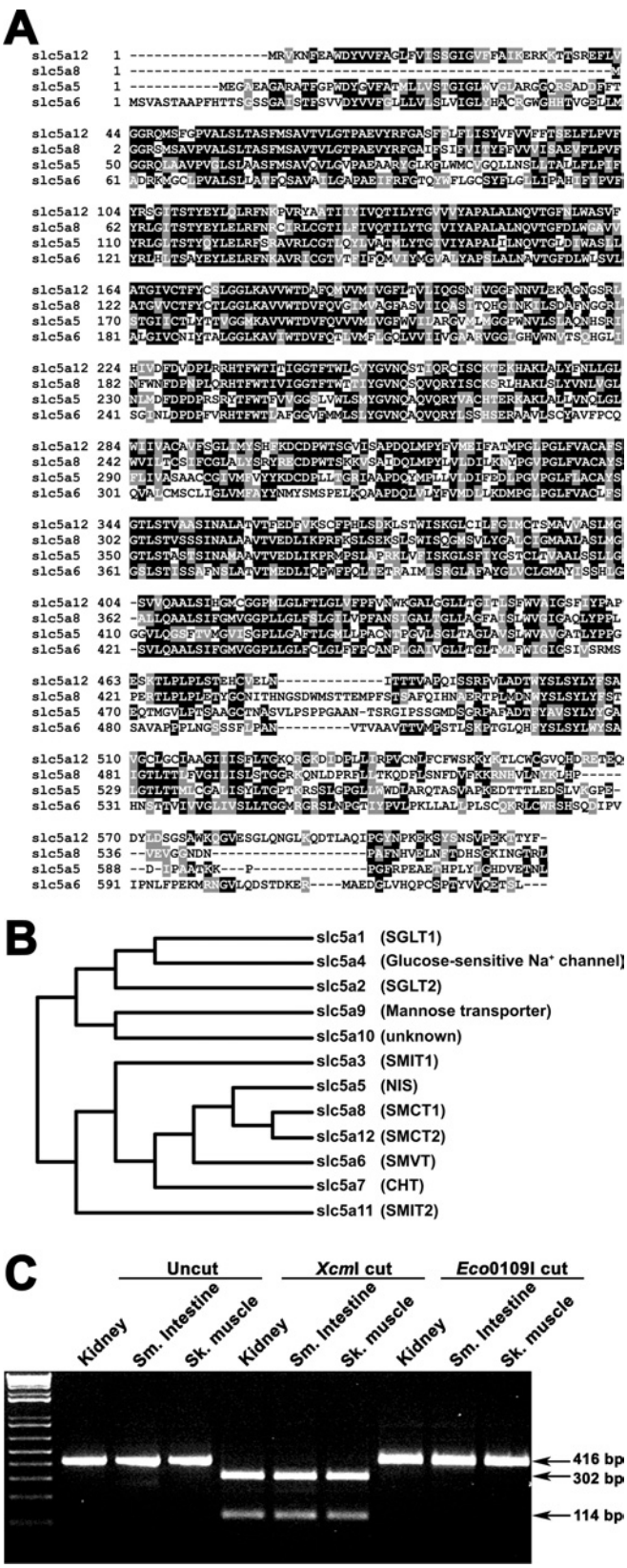

Figure 1 Structural similarity of mouse slc5a12 with other members of the *slc5* gene family and determination of the expression of slc5a12 splice variants in mouse tissues

(**A**) Alignment of amino acid sequence of mouse slc5a12 with that of mouse slc5a8 (SMCT1), mouse slc5a5 (NIS) and mouse slc5a6 (SMVT). Regions of sequence similarity are shaded.

consensus sequences for cAMP-, tyrosine kinase- and protein kinase C-dependent phosphorylation, suggesting that the transport function mediated by slc5a12 may be subject to phosphorylation-mediated regulation. Comparison of amino acid sequence between slc5a12 and slc5a8 shows a high degree of homology (59 % identity and 75 % similarity) between the two proteins. The amino acid sequence of slc5a12 also shows considerable homology with other members of the sodium-dependent glucose transporter family, particularly with slc5a5 (NIS) [26] (47 % identity and 67 % similarity) and slc5a6 (SMVT) [22] (45 % identity and 62 % similarity). The alignment of amino acid sequences of slc5a12, slc5a8, slc5a5 and slc5a6 is shown in Figure 1(A). The relationship of slc5a12 to other members of the mouse *slc5* gene family is shown by the phylogenetic tree (Figure 1B). A possible functional similarity between slc5a12 and slc5a8 is suggested from the clustering of these two transporters in one branch of the phylogenetic tree.

A BLAST search indicated that the GenBank® database contains a recently annotated entry for mouse slc5a12 with the accession no. NM_001003915. Comparison of the amino acid sequence derived from our cDNA with the predicted amino acid sequence of NM_001003915 showed that the two sequences were identical except for a stretch of 26 amino acids between positions 409 and 434 in our sequence being replaced by 27 amino acids between positions 409 and 435 in the GenBank® entry NM_001003915. Further analysis with BLAST searches against the mouse genomic sequence database indicated that the difference between the two slc5a12 sequences is due to potential alternative splicing. Alignment of both slc5a12 cDNA sequences with the mouse genomic sequence NT_039207 using the alignment tool Spidey showed the presence of a total of 15 exons, but with two alternative exon 11s. Each of the predicted exons has putative conserved donor and acceptor sequences at the splice sites. To investigate the possibility of tissue-specific expression of the splice variants, sense (5′-accagaccagctgatgccatatt-3′) and antisense (5′-ccacccagaatgacaacgtgat-3′) primers that would amplify a 416 bp fragment with an internal XcmI restriction site, corresponding to the splice variant that we report in the present study (nt 948–1363) and/or a 428 bp fragment with an internal Eco0109I restriction site, corresponding to the GenBank® splice variant (nt 1253–1680), were used in RT–PCR to amplify exon 11 along with the flanking regions of exons 10 and 12 of the two splice variants. Since tissue expression studies showed that slc5a12 is expressed only in the kidney, small intestine and skeletal muscle (see below), RNA isolated from these tissues was used in the analysis. The RT–PCR product obtained was digested with either XcmI or Eco0109I and the DNA fragments were visualized by ethidium bromide staining following size fractionation on an agarose gel. As seen in Figure 1(C), amplification product of the expected size was obtained in all three tissues. Exposure of the amplification product to XcmI resulted in the complete digestion of the PCR product to yield DNA fragments of the expected size, suggesting that the splice variant that we report in the present study is expressed in these tissues. The absence of any uncut PCR product following XcmI digestion suggests

(**B**) Phylogenetic tree of the mouse *slc5* gene family. Phylogenetic relationships between the members of the mouse *slc5* gene family were determined by multiple sequence alignments of the amino acid sequences using the CLUSTAL W algorithm [39] and the rectangle cladogram was drawn using PhyloDraw [40]. CHT, choline transporter.(**C**) Total RNA isolated from mouse kidney, small intestine and skeletal muscle was used to amplify exon 11 of slc5a12 along with adjacent regions of exons 10 and 12 by RT–PCR. The amplification products obtained were digested individually with either XcmI or Eco0109I after which they were size-fractionated on an agarose gel and stained with ethidium bromide.

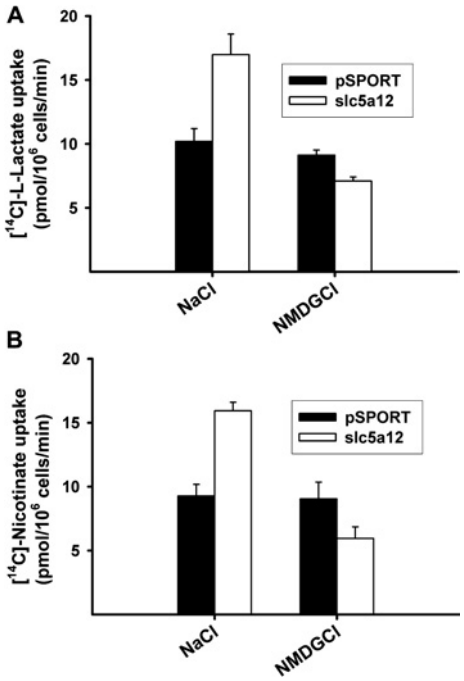

Figure 2 Functional expression of mouse slc5a12 in HRPE cells

HRPE cells were transfected with either pSPORT1 vector alone (solid bars) or mouse slc5a12 cDNA (open bars). Uptake of [^{14}C]lactate (30 μM) (**A**) and [^{14}C]nicotinate (30 μM) (**B**) were measured in these cells in the presence (NaCl) and absence (NMDG chloride) of Na^+ using a 15 min incubation. In experiments involving the measurements of lactate uptake, 5 mM α-cyano-4-hydroxycinnamate was included in the uptake buffer to block MCT-mediated lactate uptake.

that the GenBank® splice variant is not expressed. This was further corroborated by the results of Eco0109I digestion, which failed to show any detectable digestion of the PCR product. These results conclusively demonstrate that the GenBank® entry NM_001003915 is wrongly annotated and does not exist physiologically.

Functional characterization of slc5a12 following expression in HRPE cells

We assessed the transport function of slc5a12 in a heterologous expression system in HRPE cells using the vaccinia virus expression technique. Since the high degree of structural homology between slc5a12 and slc5a8 and the clustering of the two transporters in one branch in the phylogenetic tree suggested a potential functional overlap, we examined the ability of slc5a12 to mediate the transport of compounds that are known to be the substrates for slc5a8. Uptake of lactate (30 μM) was first measured in vector-transfected cells (control) and slc5a12 cDNA-transfected cells in the presence and absence of Na^+ (Figure 2A). The uptake of lactate was significantly higher in cDNA-transfected cells than in control cells when the measurement was made in the presence of Na^+. The cDNA-induced increase in uptake was 70 % [cDNA, 17.0 ± 1.6 pmol $\cdot$ (10^6 cells)$^{-1}$ $\cdot$ min^{-1}; vector, 10.2 ± 1.0 pmol $\cdot$ (10^6 cells)$^{-1}$ $\cdot$ min^{-1}]. When uptake measurements were done in the absence of Na^+, uptake of lactate in cells expressing slc5a12 was 7.1 ± 0.3 pmol $\cdot$ (10^6 cells)$^{-1}$ $\cdot$ min^{-1} compared with 9.1 ± 0.4 pmol $\cdot$ (10^6 cells)$^{-1}$ $\cdot$ min^{-1} in control cells. Similar results were obtained when nicotinate (30 μM) was used as the substrate (Figure 2B). The increase in nicotinate uptake in cDNA-transfected cells was 70 % when the measurements were made in the presence of Na^+ [cDNA, 15.9 ± 0.7 pmol $\cdot$ (10^6 cells)$^{-1}$ $\cdot$ min^{-1}; vector, 9.3 ± 0.9 pmol $\cdot$ (10^6 cells)$^{-1}$ $\cdot$ min^{-1}]. In Na^+-free buffer, nicotinate uptake was 6.0 ± 0.9 pmol $\cdot$ (10^6 cells)$^{-1}$ $\cdot$ min^{-1} in cDNA-transfected cells and 9.1 ± 1.3 pmol $\cdot$ (10^6 cells)$^{-1}$ $\cdot$ min^{-1} in vector-transfected cells. The increased uptake of lactate and nicotinate in the presence of Na^+ in slc5a12-expressing cells indicates that the slc5a12-encoded protein mediates Na^+-dependent transport of these two monocarboxylates. Interestingly, the uptake of both substrates was lower in slc5a12-expressing cells than in control cells when monitored in the absence of Na^+. It seems that these substrates may enter the cells by diffusion and Na^+-independent transport processes and that slc5a12 mediates the efflux of these substrates from the cells in the absence of extracellular Na^+. Such an efflux is likely because of the presence of an outwardly directed Na^+ gradient under these experimental conditions.

Table 2 Inhibition of slc5a12-mediated nicotinate transport by monocarboxylates

HRPE cells were transfected with one among pSPORT1 vector, slc5a12 cDNA and slc5a8 cDNA. Uptake of [^{14}C]nicotinate (30 μM) was measured in parallel in the absence or presence of unlabelled nicotinate or other monocarboxylates at the concentrations indicated. Uptake values obtained in vector-transfected cells were subtracted from corresponding uptake values obtained in cDNA-transfected cells to calculate cDNA-specific uptake. Results shown (means $\pm$ S.E.M.) represent only cDNA-specific uptake. The values in parentheses represent the percentage of control uptake (100 %) measured in the absence of inhibitors.

	[^{14}C]Nicotinate uptake [pmol $\cdot$ (10^6 cells)$^{-1}$ $\cdot$ min^{-1}]		
	slc5a12		slc5a8
Competitor	5 mM	40 mM	5 mM
Control	9.2 ± 0.3 (100)	9.5 ± 0.8 (100)	43.4 ± 2.0 (100)
Nicotinate	8.0 ± 0.8 (87)	3.3 ± 0.3 (35)	16.9 ± 0.7 (39)
Lactate	8.0 ± 0.7 (87)	4.1 ± 0.1 (43)	15.6 ± 0.05 (36)
Pyruvate	8.0 ± 0.2 (87)	3.2 ± 0.2 (34)	16.5 ± 0.7 (38)
Acetate	7.7 ± 0.9 (83)	6.3 ± 0.7 (66)	30.9 ± 2.7 (71)
Propionate	7.0 ± 0.5 (76)	3.1 ± 0.4 (32)	13.8 ± 0.5 (32)
Butyrate	6.3 ± 0.4 (69)	2.6 ± 0.2 (28)	11.1 ± 0.1 (25)
β-Hydroxybutyrate	10.5 ± 0.4 (114)	3.9 ± 0.8 (42)	18.4 ± 1.1 (42)

We next examined the substrate specificity of slc5a12-mediated transport process by competition studies in which we assessed the ability of various unlabelled monocarboxylates, including the ketone body β-hydroxybutyrate, to inhibit slc5a12-specific [^{14}C]nicotinate (30 μM) uptake. These studies were done using two concentrations of each inhibitor, 5 and 40 mM. Parallel measurements were done in cells transfected with pSPORT1 vector and the uptake values obtained in these cells were deducted from the values obtained from the corresponding cDNA-transfected cells to determine the cDNA-specific uptake. The data obtained are presented in Table 2. At a concentration of 5 mM, the maximal inhibition seen with any of the monocarboxylates was approx. 30 %. When the concentration was increased to 40 mM, the inhibition increased. Except for acetate, all other monocarboxylates (lactate, nicotinate, pyruvate, propionate and butyrate) caused >50 % inhibition under these conditions. At 5 mM, β-hydroxybutyrate did not inhibit slc5a12-mediated nicotinate uptake; however, this monocarboxylate inhibited nicotinate uptake by approx. 60 % at 40 mM. These data show that slc5a12 interacts with these substrates, including the ketone body β-hydroxybutyrate, with low affinity. For comparison, we examined, under identical experimental conditions, the efficacy of these monocarboxylates to inhibit the transport process mediated by slc5a8, a high-affinity transporter for these monocarboxylates. At a concentration of 5 mM, all monocarboxylates (except acetate), including β-hydroxybutyrate, caused >50 % inhibition

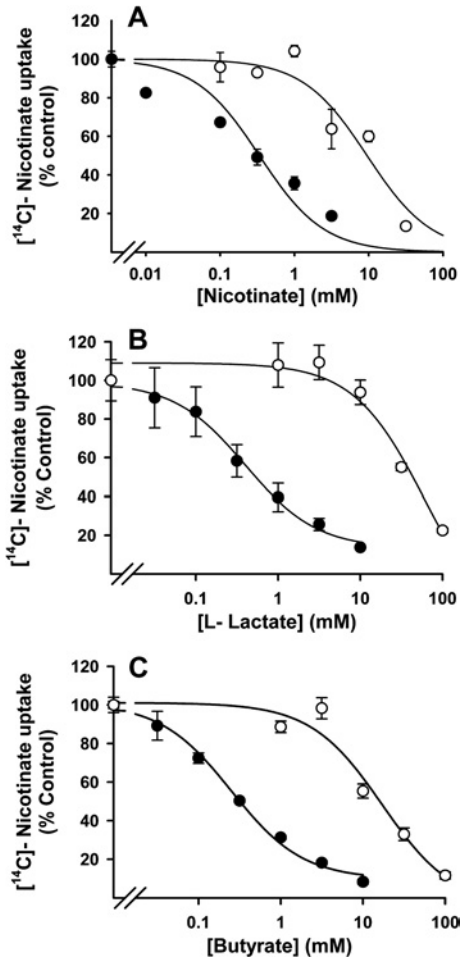

Figure 3 Dose–response relationship for the inhibition of slc5a12- and slc5a8-mediated [^{14}C]nicotinate uptake by nicotinate (A), lactate (B) and butyrate (C)

Mouse slc5a12 (open circles) and slc5a8 (filled circles) cDNAs were expressed in HRPE cells. Uptake of [^{14}C]nicotinate (30 μM) was measured with a 15 min incubation in Na^+-containing buffer in the presence of increasing concentrations of unlabelled nicotinate, lactate or butyrate. Uptake measurements made simultaneously in cells transfected with vector alone were subtracted from corresponding uptake measurements made in cells transfected with cDNA to calculate cDNA-specific uptake. Results are expressed as percentage of control uptake (100 %) measured in the absence of inhibitors.

of nicotinate uptake mediated by slc5a8. These studies show that slc5a12 is a low-affinity transporter for monocarboxylates and that slc5a8 is a high-affinity transporter for similar substrates.

We next compared the affinities of slc5a12 and slc5a8 for nicotinate, lactate and butyrate by dose–response studies. Uptake of [^{14}C]nicotinate (30 μM) was measured in slc5a12 cDNA-, slc5a8 cDNA- and pSPORT 1-transfected cells in the presence of increasing concentrations of either nicotinate, lactate or butyrate. The cDNA-specific uptake was calculated by subtracting the uptake values measured in vector-transfected cells from the values measured in cDNA-transfected cells. All three compounds inhibited slc5a12- and slc5a8-mediated uptake of radiolabelled nicotinate in a dose-dependent manner (Figure 3). However, while slc5a8-mediated [^{14}C]nicotinate uptake was inhibited at much lower concentrations of nicotinate (Figure 3A), lactate (Figure 3B) and butyrate (Figure 3C), the inhibition of slc5a12-mediated [^{14}C]nicotinate uptake occurred at much higher concentrations, confirming that slc5a12 has relatively a much lower affinity for lactate and butyrate compared with slc5a8. The IC_{50} values (i.e.

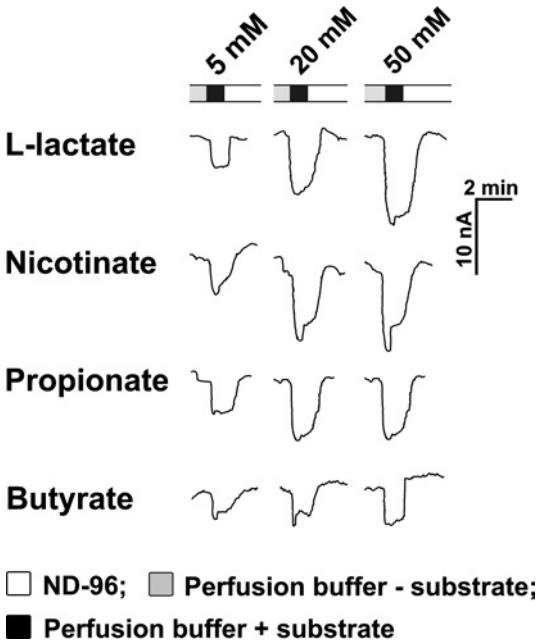

Figure 4 Substrate-induced currents in *X. laevis* oocytes expressing mouse slc5a12

Representative chart recordings of inward currents induced by increasing concentrations of lactate, nicotinate, propionate and butyrate in oocytes expressing mouse slc5a12 are shown. The currents were monitored in the presence of NaCl using the two-microelectrode voltage-clamp technique.

concentrations of inhibitors causing 50 % inhibition) calculated for nicotinate from the dose–response curve were 9.5 ± 3 mM for slc5a12-mediated uptake and 0.26 ± 0.14 mM for slc5a8-mediated uptake. Corresponding values for lactate and butyrate were 49 ± 2 and 16 ± 4 mM respectively, for slc5a12-mediated uptake, and 0.60 ± 0.02 and 0.30 ± 0.01 mM respectively, for slc5a8-mediated uptake. It is therefore apparent that the affinities of slc5a12 for nicotinate, lactate and butyrate are approx. 35-fold, approx. 80-fold and approx. 50-fold lower respectively than those of slc5a8.

Functional characterization of slc5a12 following expression in *X. laevis* oocytes

Due to the low affinity and low expression of the slc5a12 cDNA in the mammalian cell-expression system, a more detailed characterization of the slc5a12-mediated transport process using this expression system was difficult. We therefore explored the utility of the *Xenopus* oocyte expression system for characterization of slc5a12. Since slc5a12 mediates the transport of monocarboxylates by a process coupled with Na^+ as does slc5a8, we suspected that the slc5a12-mediated transport process may be electrogenic as is the case for slc5a8. Therefore we employed the two-microelectrode voltage-clamp technique to monitor the transport process. Oocytes were injected with slc5a12 cRNA and, on day 5 post-injection, substrate-induced currents were monitored in the presence of Na^+. Perfusion of oocytes with buffers containing lactate, nicotinate, propionate and butyrate elicited inward currents in oocytes expressing slc5a12 (Figure 4). Identical experiments done with water-injected oocytes did not produce any current (results not shown). The currents generated by these substrates at a concentration of 5 mM were low (2–3 nA). The magnitude of the currents, however, kept increasing with increasing concentrations of the substrates and did not

completely reach a plateau even at the highest concentration of the substrates used. The currents generated by the four substrates were 2–3 nA at 5 mM, 4–8 nA at 20 mM and 5–12 nA at 50 mM. Even when the concentration of the substrates was 50 mM, there was no evidence of complete saturation of induced currents, clearly showing the low-affinity nature of the transport process. Since the substrate-induced currents were low, further characterization of the transport process was not feasible even with this expression system.

To determine if the substrate-induced currents were comparable with the transporter-mediated substrate influx, we conducted radiotracer uptake studies in slc5a12-expressing oocytes and compared it with substrate-induced currents obtained in the studies mentioned above. Uptake of [^{14}C]lactate (5 mM) was measured in water-injected and cRNA-injected oocytes on day 5 following injection. In two independent oocyte preparations from different frogs, the slc5a12-specific uptake of lactate was 109 ± 8 and 35 ± 7 pmol · oocyte^{-1} · h^{-1}. Considering that 1 A = 1 C/s and 1 C = $1/9.65 \times 10^{-4}$ mol of charge, 5 mM lactate that generated a current of 10 nA should result in an uptake of 37.3 pmol · oocyte^{-1} · h^{-1} when one charge is co-transported with every molecule of lactate. The values for lactate uptake in radiotracer uptake studies in slc5a12-expressing oocytes are in close approximation to the predicted value. It has to be noted here, however, that the tracer uptake measurements were made without clamping the oocytes, whereas electrophysiological measurements were made under voltage-clamp conditions. Nonetheless, the substrate flux is very close to the value predicted from substrate-induced currents. This suggests that the stoichiometry of slc5a12-mediated lactate transport is 1 lactate:2 Na^+ ions, resulting in the net transfer of one positive charge.

Tissue distribution of slc5a12 mRNA

First, we used a commercially available blot for Northern-blot analysis to determine the tissue expression pattern of slc5a12. This blot contained mRNA from eight different tissues (brain, heart, kidney, liver, lung, skeletal muscle, spleen and pancreas). We could not detect the hybridization signals in any of these tissues, indicating that slc5a12 mRNA in these tissues is below detectable levels under the experimental conditions employed. When the exposure time was increased (1 week), a faint hybridization signal, 5.4 kb in size, was detectable in the kidney. We then used a Northern blot prepared in our laboratory with mRNA samples from mouse small intestine and colon. With this blot, slc5a12 transcripts were detectable in the small intestine but not in the colon (Figure 5A). Two transcripts were detected, a major 5.4 kb transcript and a minor 4.5 kb transcript. Because of the low expression of slc5a12 mRNA in all of these tissues, we used RT–PCR to analyse the tissue expression pattern for this transporter. Total RNA isolated from mouse brain, heart, kidney, liver, lung, skeletal muscle, spleen, small intestine and colon was reverse transcribed and subjected to 35 cycles of amplification in multiplexed PCR reactions with primers specific for either slc5a12 or slc5a8 and HPRT1. As seen in Figure 5(B), the slc5a12-specific amplification product was obtained in kidney, small intestine and skeletal muscle. No amplification product was detectable in the brain, heart, liver, lung, spleen and colon. In contrast, the slc5a8-specific amplification product was obtained in all tissues except the spleen. These results show that the tissue expression of slc5a12 is more limited than that of slc5a8 in the mouse.

Regional distribution of slc5a12 in the kidney and intestine

The distribution pattern of slc5a12 expression in the mouse kidney was determined by *in situ* hybridization in sagittal sections of the

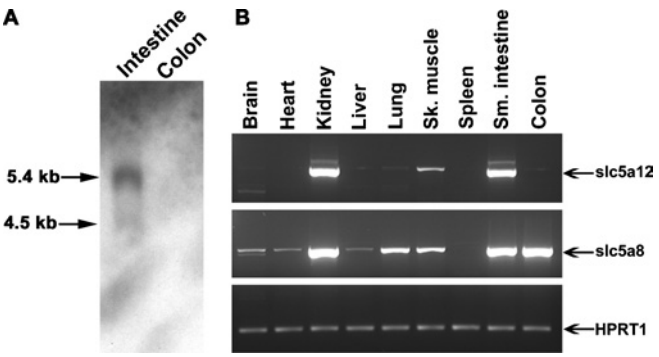

Figure 5 Expression pattern of slc5a12 in mouse tissues determined by Northern-blot analysis (A) and RT–PCR (B)

(**A**) Northern blot containing 5 μg of poly(A)$^+$ RNA from small intestine and colon was probed with an [α-^{32}P]dCTP-labelled slc5a12-specific cDNA fragment. The hybridization and post-hybridization washes were performed under high-stringency conditions. The sizes of the hybridizing RNA were determined using RNA size standards run in parallel in an adjacent lane. (**B**) Total RNA was isolated from different mouse tissues and reverse-transcribed into cDNA. RT–PCR was done using primers specific for mouse slc5a12 and slc5a8 along with primers for mouse HPRT1 (internal control) in multiplexed PCR reactions. The amplification products were size-fractionated on agarose gels and stained with ethidium bromide.

kidney (Figure 6A). Positive signals with the antisense riboprobe were observed predominantly in the cortical regions. The signals in the medullary region were faint compared with those in the cortical region. Sense riboprobe did not yield any detectable signal, demonstrating the specificity of the signal obtained with the antisense probe. At higher magnifications of the cortical and medullary regions, it was evident that the expression of slc5a12 was restricted to tubular epithelial cells. The presence of more intense staining in the epithelial cells of the outer cortical region compared with the inner cortical and medullary regions suggested that slc5a12 is expressed at higher levels in the convoluted portions of the proximal tubule (pars convoluta) than in the straight portions of the proximal tubule (pars recta).

The distribution of slc5a12 expression along the length of the intestinal tract in mouse was determined by semi-quantitative RT–PCR (Figure 6B). For comparison, semi-quantitative RT–PCR was also set up for slc5a8. The entire length of the small intestine was divided into three equal-length segments. Segment I consisted predominantly of duodenum and proximal jejunum, segment II of distal jejunum and proximal ileum and segment III of distal ileum. Caecum and colon were also used in the analysis. As seen in Figure 6(B), slc5a12 amplification product was obtained only from RNA derived from the segments of the small intestine and not from caecum and colon. Furthermore, the amount of amplification product obtained, as determined by the intensity of ethidium bromide-stained bands, was highest in the intestinal segment I and progressively decreased in segment II and in segment III. The amount of HPRT1 amplification product remained the same in all the segments, suggesting that there was no significant difference in the quality and quantity of the RNA from the different intestinal segments. From these results, it is clear that slc5a12 expression is highest in the proximal part of the small intestine and gradually decreased towards the distal end with no detectable expression in the caecum and colon. This corroborates the results from a previous Northern-blot analysis and RT–PCR that showed slc5a12 expression being restricted to the small intestine. Interestingly, the expression pattern of slc5a8 was quite different. Expression was almost undetectable in segment I of the small intestine. The expression increased gradually from segment II to distal parts of the intestinal tract.

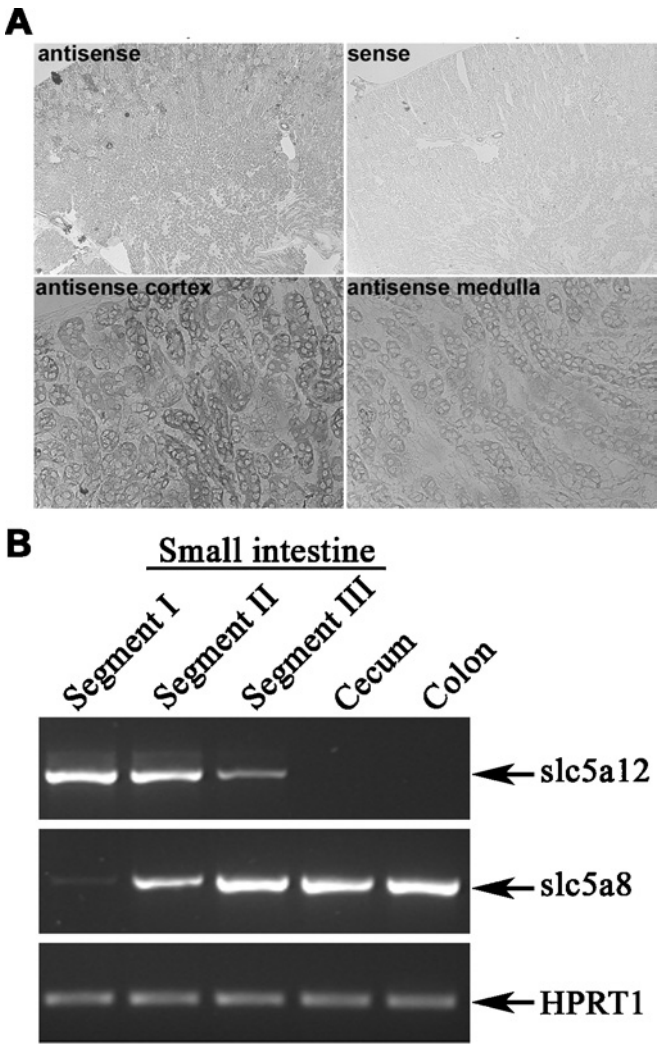

Figure 6 Regional distribution of slc5a12 transcripts assessed by *in situ* hybridization in mouse kidney (A) and by semi-quantitative RT–PCR in mouse intestinal tract (B)

(**A**) Sagittal sections of mouse kidney were hybridized with slc5a12-specific antisense and sense (negative control) riboprobes. Staining obtained with antisense probe in the cortex and medulla is shown at higher magnification to demonstrate the localization of the hybridization signal in tubular cells. (**B**) Mouse small intestine was dissected and cut into three equal-length segments. Total RNA was isolated from these three segments and also from the caecum and colon. RT–PCR was done using primers specific for mouse slc5a12 and slc5a8 along with primers for mouse HPRT1 (internal control) in multiplexed PCR reactions using 300 pmol of each primer and 25 cycles of amplification. The amplification products were size-fractionated on agarose gels and stained with ethidium bromide.

More importantly, slc5a8 expression was maximal in the caecum and colon. Thus the expression of slc5a12 is restricted to the proximal portions of the mouse intestinal tract with predominant expression in the small intestine, whereas the expression of slc5a8 is restricted comparatively to the distal portions of the intestinal tract with predominant expression in the large intestine.

DISCUSSION

Functional characteristics of mouse slc5a12

Until recently, the solute carrier gene family *SLC5* was believed to contain only 11 members [1,2]. In the present paper, we report on the cloning and functional identification of the twelfth member of this gene family. Functional studies have shown that slc5a12 serves as a low-affinity Na^+-coupled transporter for short-chain monocarboxylates, such as lactate, nicotinate, short-chain fatty acids and β-hydroxybutyrate. The substrate specificity of slc5a12 is strikingly similar to that of slc5a8. However, slc5a12 interacts with its substrates with relatively lower affinity, whereas slc5a8 interacts with its substrates with a much higher affinity. Based on these functional features, we rename slc5a8 as SMCT1 (instead of SMCT) and designate the newly identified slc5a12 as SMCT2. To determine if any other high-affinity substrate exists for SMCT2, we screened several compounds. The list included glucose, biotin, pantothenate, mannose, *myo*-inositol, choline and iodide. None of these compounds was found to be a substrate for SMCT2 (results not shown).

The existence of two distinct transport systems for lactate and other short-chain fatty acids in the kidney tubular brush border membrane has been reported [20,27]. While the membrane vesicles isolated from pars recta (inner cortical and outer medullary regions) possessed a high-affinity lactate transporter, the membrane vesicles isolated from pars convoluta (outer cortical region) possessed a low-affinity lactate transporter. Since slc5a8 has high affinity for lactate, it is most likely responsible for the high-affinity transport system. This is in agreement with our findings that slc5a8 expression is readily detectable in the medullary region of the kidney [15]. slc5a12 expression is maximal in the cortical region of the kidney where the low-affinity lactate transport system is found. Therefore slc5a12 is likely to represent the low-affinity system.

Tosco et al. [28] have reported on the presence of an endogenous Na^+-dependent monocarboxylate transport system that can mediate the transport of lactate and pyruvate in *X. laevis* oocytes. In the present study, we could neither detect substrate-induced currents nor Na^+-dependent lactate uptake in water-injected oocytes. Since Tosco et al. [28] used 2 day-old oocytes in their studies and we used 5 day-old oocytes, the difference in the results of the two studies is likely to be due to differences in the experimental conditions. Therefore we measured the endogenous lactate uptake on day 2 following oocyte isolation. These studies showed that there was a significant increase in lactate uptake ($\sim$30 %) when measured in the presence of Na^+ compared with uptake measured in the absence of Na^+. These data corroborate the results of Tosco et al. [28]. Thus *X. laevis* oocytes express SMCT-like transport activity endogenously when measured on day 2 after isolation, but the activity disappears if the oocytes are maintained for longer periods.

Tissue distribution and physiological role of SMCT2

Among the tissues examined, the expression of SMCT2 is limited only to three tissues: kidney, small intestine and skeletal muscle. In the kidney, SMCT2 is expressed in the early portions of the proximal tubule, whereas SMCT1 is expressed in the latter portions. Plasma concentrations of lactate are in the range 1–1.5 mM [21]. The levels increase significantly in situations such as exercise, hypoxia, anaemia and mitochondrial disorders. Therefore the proximal portions of the nephron are exposed to high concentrations of lactate. A low-affinity transport system is appropriate to mediate effective absorption of lactate at these high concentrations. As reabsorption continues along the proximal tubule, lactate concentrations decrease significantly and therefore a high-affinity transport system would be better suited to mediate effective absorption at these lower concentrations in the latter parts of the proximal tubule. Thus the differential distribution of the low-affinity transporter SMCT2 in the early parts of the proximal tubule and the high-affinity transporter SMCT1 in the

latter parts makes sense in terms of effective absorption of lactate in the kidney. This situation is analogous to the distribution of the low-affinity peptide transporter PepT1 in the proximal regions of the proximal tubule and the high-affinity peptide transporter PepT2 in the latter regions of the proximal tubule [29].

The expression of SMCT2 in the small intestine and skeletal muscle is rather surprising. Although an Na^+-dependent transport system for lactate has been reported in the intestinal brush-border membrane [30–32], the H^+-coupled lactate transporters (MCTs) are believed to play a primary role in the intestinal absorption of lactate [33]. However, we recently reported on the expression of the high-affinity Na^+-coupled MCT, SMCT1, in the small intestine and colon [14,15]. The present studies show that the low-affinity Na^+-coupled MCT, SMCT2, is also expressed in the intestinal tract, but with a distribution pattern different from that of SMCT1. While SMCT2 is expressed predominantly in the proximal part of the small intestine and is absent from the caecum and colon, SMCT1 is expressed in the distal part of the small intestine and in the caecum and colon. The concentrations of short-chain monocarboxylates (acetate, propionate and butyrate) are high in the caecum and colon due to bacterial fermentation of dietary fibre. The expression of SMCT1 in these parts of the intestinal tract is essential for effective absorption of these bacterial metabolites. These metabolites serve as preferred energy substrates for colonocytes. The proximal regions of the small intestine, where SMCT2 is expressed, are relatively sterile with minimal bacterial colonization. It seems therefore that the physiological function of SMCT2 may be to absorb lactate and other monocarboxylates from dietary sources. Fermented milk and yoghurt contain high levels of lactate and other short-chain fatty acids. Furthermore, breast milk consists of triacylglycerols with short- and medium-chain fatty acids and therefore neonatal intestine is exposed to significant amounts of these substrates from diet. We speculate that the physiological function of SMCT2 in the proximal small intestine is to mediate the absorption of these dietary components. An Na^+-coupled transport system for lactate has been described in the intestinal brush-border membrane [30–32], but this transport process has been shown to be electroneutral. SMCT2 is also an Na^+-coupled transporter for lactate, but the transport process is electrogenic. However, we believe that SMCT2 represents the Na^+-coupled lactate transport system that has been described in the small intestine and that the discrepancy in the mechanism of the transport process is most likely due to experimental variations. We find a similar situation in the kidney. Renal brush-border membranes possess an Na^+-coupled transport system for lactate, but there is no consensus as to whether the transport process is electroneutral or electrogenic. Some studies have shown the transport process to be electroneutral [34], whereas other studies have shown the transport process to be electrogenic [19,35,36].

Skeletal muscle is generally thought to be a lactate exporter where muscle contraction leads to the generation of lactate, which is subsequently released into the circulation via MCTs. Recent studies, however, indicate that there is significant uptake and oxidative utilization of lactate in resting skeletal muscle and that lactate exchange occurs between white-glycolytic and red-oxidative fibres [37,38]. The H^+-coupled lactate transporters MCT1 and MCT4 are believed to be primarily responsible for both lactate release and uptake from and into the skeletal muscle cell. There are no reports on the presence of Na^+-dependent transport mechanisms for lactate in the skeletal muscle. Our RT–PCR results clearly demonstrate the presence of both SMCT1 and SMCT2 transcripts in the skeletal muscle. These transporters are likely to play a critical role in the handling of lactate by the skeletal muscle.

This work was supported by the National Institutes of Health grant HD37150 to P. D. P.

REFERENCES

1 Wright, E. M., Loo, D. D., Hirayama, B. A. and Turk, E. (2004) Surprising versatility of Na^+-glucose cotransporters: SLC5. Physiology (Bethesda) **19**, 370–376
2 Wright, E. M. and Turk, E. (2004) The sodium/glucose cotransport family SLC5. Pflugers Arch. **447**, 510–518
3 Hediger, M. A., Turk, E. and Wright, E. M. (1989) Homology of the human intestinal Na^+/glucose and *Escherichia coli* Na^+/proline cotransporters. Proc. Natl. Acad. Sci. U.S.A. **86**, 5748–5752
4 Wells, R. G., Pajor, A. M., Kanai, Y., Turk, E., Wright, E. M. and Hediger, M. A. (1992) Cloning of a human kidney cDNA with similarity to the sodium-glucose cotransporter. Am. J. Physiol. **263**, F459–F465
5 Berry, G. T., Mallee, J. J., Kwon, H. M., Rim, J. S., Mulla, W. R., Muenke, M. and Spinner, N. B. (1995) The human osmoregulatory Na^+/myo-inositol cotransporter gene (SLC5A3): molecular cloning and localization to chromosome 21. Genomics **25**, 507–513
6 Roll, P., Massacrier, A., Pereira, S., Robaglia-Schlupp, A., Cau, P. and Szepetowski, P. (2002) New human sodium/glucose cotransporter gene (KST1): identification, characterization, and mutation analysis in ICCA (infantile convulsions and choreoathetosis) and BFIC (benign familial infantile convulsions) families. Gene **285**, 141–148
7 Smanik, P. A., Liu, Q., Furminger, T. L., Ryu, K., Xing, S., Mazzaferri, E. L. and Jhiang, S. M. (1996) Cloning of the human sodium iodide symporter. Biochem. Biophys. Res. Commun. **226**, 339–345
8 Wang, H., Huang, W., Fei, Y. J., Xia, H., Yang-Feng, T. L., Leibach, F. H., Devoe, L. D., Ganapathy, V. and Prasad, P. D. (1999) Human placental Na^+-dependent multivitamin transporter. Cloning, functional expression, gene structure, and chromosomal localization. J. Biol. Chem. **274**, 14875–14883
9 Apparsundaram, S., Ferguson, S. M., George, Jr, A. L. and Blakely, R. D. (2000) Molecular cloning of a human, hemicholinium-3-sensitive choline transporter. Biochem. Biophys. Res. Commun. **276**, 862–867
10 Ganapathy, V., Gopal, E., Miyauchi, S. and Prasad, P. D. (2005) Biological functions of SLC5A8, a candidate tumour suppressor. Biochem. Soc. Trans. **33**, 237–240
11 Tazawa, S., Yamato, T., Fujikura, H., Hiratochi, M., Itoh, F., Tomae, M., Takemura, Y., Maruyama, H., Sugiyama, T., Wakamatsu, A. et al. (2005) SLC5A9/SGLT4, a new Na^+-dependent glucose transporter, is an essential transporter for mannose, 1,5-anhydro-D-glucitol, and fructose. Life Sci. **76**, 1039–1050
12 Diez-Sampedro, A., Hirayama, B. A., Osswald, C., Gorboulev, V., Baumgarten, K., Volk, C., Wright, E. M. and Koepsell, H. (2003) A glucose sensor hiding in a family of transporters. Proc. Natl. Acad. Sci. U.S.A. **100**, 11753–11758
13 Coady, M. J., Chang, M. H., Charron, F. M., Plata, C., Wallendorff, B., Sah, J. F., Markowitz, S. D., Romero, M. F. and Lapointe, J. Y. (2004) The human tumour suppressor gene SLC5A8 expresses a Na^+-monocarboxylate cotransporter. J. Physiol. (Cambridge, U.K.) **557**, 719–731
14 Gopal, E., Fei, Y. J., Miyauchi, S., Zhuang, L., Prasad, P. D. and Ganapathy, V. (2005) Sodium-coupled and electrogenic transport of B-complex vitamin nicotinic acid by slc5a8, a member of the Na/glucose cotransporter gene family. Biochem. J. **388**, 309–316
15 Gopal, E., Fei, Y. J., Sugawara, M., Miyauchi, S., Zhuang, L., Martin, P., Smith, S. B., Prasad, P. D. and Ganapathy, V. (2004) Expression of slc5a8 in kidney and its role in Na^+-coupled transport of lactate. J. Biol. Chem. **279**, 44522–44532
16 Miyauchi, S., Gopal, E., Fei, Y. J. and Ganapathy, V. (2004) Functional identification of SLC5A8, a tumor suppressor down-regulated in colon cancer, as a Na^+-coupled transporter for short-chain fatty acids. J. Biol. Chem. **279**, 13293–13296
17 Poole, R. C. and Halestrap, A. P. (1993) Transport of lactate and other monocarboxylates across mammalian plasma membranes. Am. J. Physiol. **264**, C761–C782
18 Wright, E. M. (1985) Transport of carboxylic acids by renal membrane vesicles. Annu. Rev. Physiol. **47**, 127–141
19 Barac-Nieto, M., Murer, H. and Kinne, R. (1980) Lactate-sodium cotransport in rat renal brush border membranes. Am. J. Physiol. **239**, F496–F506
20 Jorgensen, K. E. and Sheikh, M. I. (1984) Renal transport of monocarboxylic acids. Heterogeneity of lactate-transport systems along the proximal tubule. Biochem. J. **223**, 803–807
21 Craig, F. N. (1946) Renal tubular reabsorption, metabolic utilization, and isomeric fractionation of lactic acid in the dog. Am. J. Physiol. **146**, 146–159
22 Prasad, P. D., Wang, H., Kekuda, R., Fujita, T., Fei, Y. J., Devoe, L. D., Leibach, F. H. and Ganapathy, V. (1998) Cloning and functional expression of a cDNA encoding a mammalian sodium-dependent vitamin transporter mediating the uptake of pantothenate, biotin, and lipoate. J. Biol. Chem. **273**, 7501–7506

23 Kekuda, R., Prasad, P. D., Wu, X., Wang, H., Fei, Y. J., Leibach, F. H. and Ganapathy, V. (1998) Cloning and functional characterization of a potential-sensitive, polyspecific organic cation transporter (OCT3) most abundantly expressed in placenta. J. Biol. Chem. **273**, 15971–15979
24 Halestrap, A. P. and Meredith, D. (2004) The SLC16 gene family – from monocarboxylate transporters (MCTs) to aromatic amino acid transporters and beyond. Pflugers Arch. **447**, 619–628
25 Halestrap, A. P. and Price, N. T. (1999) The proton-linked monocarboxylate transporter (MCT) family: structure, function and regulation. Biochem. J. **343**, 281–299
26 Pinke, L. A., Dean, D. S., Bergert, E. R., Spitzweg, C., Dutton, C. M. and Morris, J. C. (2001) Cloning of the mouse sodium iodide symporter. Thyroid **11**, 935–939
27 Jorgensen, K. E. and Sheikh, M. I. (1986) Characteristics of uptake of short chain fatty acids by luminal membrane vesicles from rabbit kidney. Biochim. Biophys. Acta **860**, 632–640
28 Tosco, M., Orsenigo, M. N., Gastaldi, G. and Faelli, A. (2000) An endogenous monocarboxylate transport in *Xenopus laevis* oocytes. Am. J. Physiol. **278**, R1190–R1195
29 Shen, H., Smith, D. E., Yang, T., Huang, Y. G., Schnermann, J. B. and Brosius, III, F. C. (1999) Localization of PEPT1 and PEPT2 proton-coupled oligopeptide transporter mRNA and protein in rat kidney. Am. J. Physiol. **276**, F658–F665
30 Hildmann, B., Storelli, C., Haase, W., Barac-Nieto, M. and Murer, H. (1980) Sodium ion/L-lactate co-transport in rabbit small-intestinal brush-border-membrane vesicles. Biochem. J. **186**, 169–176
31 Storelli, C., Corcelli, A., Cassano, G., Hildmann, B., Murer, H. and Lippe, C. (1980) Polar distribution of sodium-dependent and sodium-independent transport system for L-lactate in the plasma membrane of rat enterocytes. Pflugers Arch. **388**, 11–16
32 Wolffram, S., Grenacher, B. and Scharrer, E. (1988) Sodium-dependent L-lactate uptake by bovine intestinal brush border membrane vesicles. J. Dairy Sci. **71**, 3267–3273
33 Tamai, I., Sai, Y., Ono, A., Kido, Y., Yabuuchi, H., Takanaga, H., Satoh, E., Ogihara, T., Amano, O., Izeki, S. et al. (1999) Immunohistochemical and functional characterization of pH-dependent intestinal absorption of weak organic acids by the monocarboxylic acid transporter MCT1. J. Pharm. Pharmacol. **51**, 1113–1121
34 Barbarat, B. and Podevin, R. A. (1988) Stoichiometry of the renal sodium-L-lactate cotransporter. J. Biol. Chem. **263**, 12190–12193
35 Mengual, R., Claude-Schlageter, M. H., Poiree, J. C., Yagello, M. and Sudaka, P. (1989) Characterization of sodium and pyruvate interactions of the two carrier systems specific of mono- and di- or tricarboxylic acids by renal brush-border membrane vesicles. J. Membr. Biol. **108**, 197–205
36 Mengual, R., Schlageter, M. H. and Sudaka, P. (1990) Kinetic asymmetry of renal Na^+-L-lactate cotransport. Characteristic parameters and evidence for a ping pong mechanism of the trans-stimulating exchange by pyruvate. J. Biol. Chem. **265**, 292–299
37 Brooks, G. A. (2002) Lactate shuttles in nature. Biochem. Soc. Trans. **30**, 258–264
38 Juel, C. (2001) Current aspects of lactate exchange: lactate/H^+ transport in human skeletal muscle. Eur. J. Appl. Physiol. **86**, 12–16
39 Thompson, J. D., Higgins, D. G. and Gibson, T. J. (1994) CLUSTAL W: improving the sensitivity of progressive multiple sequence alignment through sequence weighting, position-specific gap penalties and weight matrix choice. Nucleic Acids Res. **22**, 4673–4680
40 Choi, J. H., Jung, H. Y., Kim, H. S. and Cho, H. G. (2000) PhyloDraw: a phylogenetic tree drawing system. Bioinformatics **16**, 1056–1058

Received 9 June 2005/11 August 2005; accepted 17 August 2005
Published as BJ Immediate Publication 17 August 2005, doi:10.1042/BJ20050927